Purification of Lithium Carbonate from Radioactive Contaminants Using MnO_2–Based Inorganic Sorbent

Olga Gileva *, Pabitra Arial , JunSeok Choe , Yena Kim , Yeongduk Kim , Eun Kyung Lee , Moo Hyun Lee , Vitaly Milyutin , KeonAh Shin , Hyojin Yeon

Posted Date: 8 September 2023

doi: 10.20944/preprints202309.0580.v1

Keywords: lithium carbonate; lithium nitrate; radiochemical purification; co-precipitation; membrane filtration; sorption; MnO2-based inorganic sorbent; AMoRE experiment.

Article

Purification of Lithium Carbonate from Radioactive Contaminants Using MnO_2–Based Inorganic Sorbent

Olga Gileva [1,*], Pabitra Arial [1], JunSeok Choe [1], Yena Kim [1], Yeongduk Kim [1,2], Eun Kyung Lee [1], Moo Hyun Lee [1,2], Vitaly Milyutin [3], KeonAh Shin [1] and Hyojin Yeon [1]

[1] Center for Underground Physics, Institute for Basic Science (IBS), Daejeon 34126, Korea; gilevaolga@ibs.re.kr
[2] IBS School, University of Science and Technology (UST), Daejeon 34113, Korea
[3] Froumkin's Institute of Physical Chemistry and Electrochemistry of the Russian Academy of Sciences (IPCE RAS), Moscow 119071, Russia; vmilyutin@mail.ru
* Correspondence: gilevaolga@ibs.re.kr

Abstract: The possibility of deep radiochemical purification of Li_2CO_3 has been examined in the frame of the purification program of AMoRE collaboration. In this experiment, commercial Li_2CO_3 was converted into $LiNO_3$. Co-precipitation with inorganic salt-based carriers followed by membrane filtration and sorption using MDM inorganic sorbent methods were tested for the removal of alkaline-earth and transition metals, potassium, magnesium, aluminum, uranium, thorium, and radium. The calcium molybdate-based carrier was the most efficient for removing Th, U, and K. Subsequently, the radium, calcium, and barium contaminations were removed with MDM sorbent. After the impurities' removal, the final Li_2CO_3 product was synthesized with NH_4HCO_3 sludge. The separation factors were derived by means of ICP-MS and HPGe analyses of the initial material, intermediate and final products. The study showed the optimum conditions of co-precipitation and sorption to reach a high yield and radiopurity of lithium carbonate used for low radioactive background experiments.

Keywords: lithium carbonate; lithium nitrate; radiochemical purification; co-precipitation; membrane filtration; sorption; MnO_2-based inorganic sorbent; AMoRE experiment

1. Introduction

Lithium has been historically used in various fields of science and technology, in the production of ceramic and glass materials, greases, aluminum, and others. In the pharmaceutical industry, it is used to produce medicines to treat mental disorders [1]. In nuclear and power industries, lithium is used as a heat transfer for nuclear reactors [2], in the burial of high-activity nuclear wastes [3], and for tritium control and capture in controlled thermonuclear fusion reactors [4]. Lithium and its compounds have recently been among the most demanded rare metals because of its use in the lithium battery industry [1]. In physics science, lithium targets find practical application in plasma acceleration technology [5]. In particle physics, lithium carbonate is used as a precursor for producing cryogenic bolometric lithium molybdate (LMO) crystals to detect neutrinoless double beta decay (0νDBD) of ^{100}Mo isotope. The Mo-100 isotope has a comparatively high natural abundance (9.74%) [6] and a high $Q_{\beta\beta}$-value of 3034.40(17) keV [7], while most natural radiation has energies below 2615 keV. However, the 0νDBD search is very challenging due to the exceptional rarity of these events, greater than 1.1×10^{24} yr half-lives for ^{100}Mo [8–10]. The AMoRE project is a series of experiments to search for the 0νDBD of ^{100}Mo embedded in molybdate-based bolometric crystals using low-temperature calorimeters. AMoRE-II, the second phase of the experiment, aims to probe the corresponding half-live limit $T_{1/2}^{0\nu} > 5 \times 10^{26}$ years having the radioactive background to be lower than 10^{-4} ckky at 3034 ± 10 keV [11] using an array of about 400 $Li_2{}^{100}MoO_4$ crystals. Many efforts must be made to reach the projected background and sensitivity levels. First of all, radioactive contamination from ^{40}K, ^{226}Ra, ^{238}U, and ^{228}Th naturally existing inside the crystals must be reduced to minimize the contribution to the background level. Bolometers for AMoRE-II are produced with

 doi:10.20944/preprints202309.0580.v1

conventional [12] and low-temperature gradient Czochralski [13] techniques. To ensure the grown crystals' radiopurity and uniformity despite the crystallization technique used, high-purity and low-radioactive initial materials, $^{100}MoO_3$ [14] and Li_2CO_3 powders, are required for crystal synthesis. The presented study mainly focuses on the Li_2CO_3 preparation for the AMoRE project. Taking into account the segregation of radio impurities during the crystal growth [12], the ^{40}K level below 100 mBq/kg and Th/U at the level of several mBq/kg in the Li_2CO_3 precursor would be acceptable. Then, about 150 kg of this ultra-low radioactive high-purity (over 99.99%) lithium carbonate powder is required to produce 400 LMO crystals for AMoRE-II.

Commercial lithium carbonate purity is available up to 99.999% grade, raising the powder's cost to over 1000 US$/kg. For these products, the certificates of analysis (COA) issued by the producers specify the content of alkali, alkali-earth, transition, and heavy metals on ppm level and do not contain data on radioactive contamination. Moreover, the radiopurity of the powder may vary from lot to lot, but to get the powder from one dedicated tested in advance lot is almost impossible. The HPGe gamma spectrometry screening of various samples of 99.99% and 99.999% lithium carbonate powders showed high contamination in ^{226}Ra and ^{40}K from a few mBq/kg to Bq/kg [15]. Thus, developing the radiochemical purification method for producing high-purity lithium carbonate powder is a crucial issue for the AMoRE project.

The presented study is devoted to the investigation of the possibility of purifying lithium carbonate powder from lithium nitrate solutions using co-precipitation and sorption with MnO_2-based inorganic sorbent. The paper is structured as follows: materials and methods used are described in Sect. 2. The results of co-precipitation with different carriers are presented in Sect. 3. Section 4 describes the sorption purification using MnO_2 – based sorbent. Finally, Sect. 5 provides the conclusion and discussion of the results.

2. Materials and methods

Lithium nitrate purification was performed in a class 1,000 clean room (ISO6) at the Center for Underground Physics (CUP) of the Institute for Basic Science (IBS) in Korea [16]. Pharmaceutical-grade lithium carbonate powder from Novosibirsk Rare Metal Plant (Russia) [17] was selected as the initial material for a comparatively reasonable price, and the possibility of buying all required 150 kg from the same batch. Nitric acid (67 – 70%, TraceMetal grade) was purchased from Fisher Chemical™ and used without any purification for dissolving the initial Li_2CO_3 powder. Lithium hydroxide monohydrate from Sigma-Aldrich® (ACS reagent, ≥ 98.0%) was used to adjust the initial lithium nitrate solution pH. Nitric acid purified with Savillex® DST sub-boiling acid purification system and aqueous ammonium hydroxide solution supplied by Sigma-Aldrich® (~25% Puriss) were used on the final steps of purification and for pH adjustment.

A calcium-based carrier for co-precipitation was produced from commercially available calcium carbonate and purified at CUP. A calcium molybdate (CMO) based carrier was synthesized from the CUP-purified calcium carbonate and natural molybdenum trioxide powders [18] through the interaction of calcium nitrate and ammonium molybdate solutions. The carriers were introduced into the lithium nitrate solution to about 5 mol%. Following the co-precipitation with the Li_2CO_3 carrier, the initial lithium carbonate powder was taken in about 5% access amount to the required HNO_3 for complete dissolving. After the carrier was introduced, the mixture pH was adjusted with LiOH to 9, stirred well, and left overnight to let the sediment grow and settle down. The sediment was filtered out using a membrane 0.1 μm pore size PTFE filter (Advantec®, Japan).

The filtrate obtained after the membrane filtration was subjected to a sorption purification in the dynamic mode with manganese (III, IV) oxyhydrate-based MDM sorbent [19]. Prior to being used, the sorbent was precleaned and conditioned to Li-form. The sorbent was soaked in 1% HNO_3 solution to remove small dust particles, rinsed, and charged into Savillex® 120 mL volume PTFE column. The precleaning was performed by successive treatment with 3 mol L^{-1} HNO_3 followed by 0.1 mol L^{-1} HNO_3. Lithium nitrate solution with a concentration of 1 mol L^{-1} and pH 9 was used for column conditioning. The purification was performed by passing the $LiNO_3$ solution through the column at a rate of 3 bed volumes (b.v.) per hour. The solution after the column was collected in fractions, where

Preprints (www.preprints.org) | NOT PEER-REVIEWED | Posted: 8 September 2023 doi:10.20944/preprints202309.0580.v1

K, Ba, Sr, Th, and U were analyzed with ICP-MS at CUP. The results of this analysis were used to check the purification efficiency and define the separation factors. The separation factors were determined from the ratio of the initial material's impurity concentrations to those in the purified product.

The $LiNO_3$ solution received after the column purification was evaporated to reach the concentration of about 8 mol L^{-1}, filtered with a membrane 0.1 μm pore size PTFE filter (Advantec®, Japan), and the pH was lowered to about 2. The acidified solution was kept in the fridge at 4 °C overnight to force the crystallization. The $LiNO_3$ crystallohydrate was filtered under vacuum and dried. To avoid melting the product, the crystals were dried at room temperature for three days under vacuum (< 10 mTorr), and then the temperature was slowly raised to 120 °C to ensure water removal. Dry lithium nitrate powder was tested with HR-ICP-MS at SEASTAR™ [20] and HPGe gamma spectrometry at CUP [21]. Final lithium carbonate powder was synthesized through the interaction with ammonium bicarbonate sludge (Fisher Chemical™, SLR grade). Before Li_2CO_3 final synthesis, about 5% of the stoichiometric amount of NH_4HCO_3 was added into lithium nitrate saturated at 40 °C solution and mixed until a small amount of Li_2CO_3 sediment occurred. The sediment was filtered with the same membrane filter, and the synthesis was completed. Synthesized lithium carbonate powder was rinsed several times with hot deionized water and dried.

3. Lithium nitrate purification via co-precipitation

Once received from the company producer, raw lithium carbonate powder was tested to understand the level of chemical and radioactive contamination (Table 1).

Table 1. The concentration of metallic impurities (HR-ICP-MS) and radioactivity levels (HPGe) measured in initial lithium carbonate powder.

Element	Concentration [ppb]	Element	Concentration [ppb]		Activity [mBq/kg]
Al	530 ± 50	Mn	80 ± 20	^{40}K	≤ 66
B	4,800 ± 500	Na	1,720 ± 150	^{137}Cs	≤ 3
Ba	15,200 ± 1,500	Ni	230 ± 30	^{234}Th	≤ 151
Ca	36,000 ± 5,000	Pb	18 ± 2	^{234m}Pa	≤ 162
Cr	650 ± 150	Sr	310 ± 50	^{226}Ra	2730 ± 140
Cs	420 ± 50	Th232	0.09 ± 0.02	^{228}Ac	110 ± 10
Cu	120 ± 30	Ti	140 ± 20	^{228}Th	9 ± 3
Fe	1,100 ± 200	U238	1.1 ± 0.1		
K	770 ± 70	V	130 ± 20		
Mg	19,500 ± 1,500	Zn	300 ± 50		

Along with the HPGe testing, the content of alkali, alkali-earth, transition, and heavy metals was studied with HR-ICP-MS. Measurements showed unacceptable 2^{26}Ra (from the ^{238}U decay chain) and ^{228}Ac/^{228}Th (from the ^{232}Th decay chain) activities, while ^{40}K and ^{137}Cs activity levels were low enough to be used in AMoRE-II crystal synthesis. The Ca, Ba, Mg, B, Fe, and Na concentrations were over the acceptable one ppm level and must be reduced to avoid contamination of the AMoRE-II crystals. The lithium nitrate solution was selected as an intermediate compound for further purification due to the simplicity of preparing pure nitric acid and the possibility of applying it to the manganese oxide-based sorbent. Purified lithium nitrate could be converted into carbonate by interacting with NH_4HCO_3 sludge or CO_2 and NH_3 gases [22].

The initial lithium nitrate solution obtained after the complete dissolving of the raw Li_2CO_3 powder was highly colored brown, indicating high iron contamination. With increasing the pH of the solution to 9, insoluble in alkali media hydroxides occurred in the solution volume. Various carriers were introduced into the solution to force the co-precipitation of insoluble impurities. Calcium-based and carbonate-based carriers were selected for Ra removal. Our previous studies approved the CMO-based carrier [14,18] as an efficient for thorium and radium separation. After the

Preprints (www.preprints.org) | NOT PEER-REVIEWED | Posted: 8 September 2023 doi:10.20944/preprints202309.0580.v1

co-precipitate was filtered out using the PTFE membrane filter, the lithium nitrate solution was analyzed with ICP-MS at CUP (Table 2).

Table 2. Impurities reduction in lithium nitrate using the co-precipitation method of purification.

	K [ppb]	Sr [ppb]	Ba [ppb]	Ca [ppm]	Fe [ppb]	Pb [ppb]	Th [ppt]	U [ppt]
Initial material	770 ± 70	310 ± 50	15,200 ± 1,500	36 ± 5	1100 ± 200	18 ± 2	90 ± 20	1100 ± 100
Co-prec. with Li_2CO_3	430 ± 50	160 ± 30	1200 ± 150	30 ± 5	200 ± 50	10 ± 1	≤6	200 ± 30
Co-prec. with $CaCO_3$	270 ± 30	9350 ± 500	1400 ± 150	50 ± 5	200 ± 50	0.7 ± 0.2	≤6	150 ± 20
Co-prec. with $CaMoO_4$	300 ± 30	1100 ± 100	900 ± 100	45 ± 5	<100	<0.1	≤6	≤6

*The results values are normalized with $LiNO_3$ concentration.

All selected carriers were found to be efficient for the removal of measured contaminants, but the calcium molybdate showed the highest decontamination factors. Barium, used as a Ra indicator, was reduced 15 times. The uranium concentration was reduced by three orders of magnitude and thorium – by one order, resulting in the project's satisfactory limit of six ppt. The alkali potassium does not form insoluble compounds under given conditions, and the separation is possible only due to occlusion or mechanical entrapment. Measurements confirmed that the K concentration decreased twice and was found to be about 0.3 ppm. Strontium and calcium concentrations in the resulting solution were affected by cross-contamination from Ca-based carriers themselves but could be smoothed out in the following column purification. Remarkably, the removal of uranium in the presence of carbonate anion was much less efficient than CMO-based co-precipitation, which could be explained by the formation of the stable soluble uranyl carbonate complexes [23].

4. Lithium nitrate sorption purification

The lithium nitrate solution after CMO-based co-precipitation was forwarded to sorption purification using MDM sorbent. The impurities removal rate was tested for 1 mol L^{-1}, 4 mol L^{-1}, and 7 mol L^{-1} $LiNO_3$ solution at pH 8. About 50 column volumes of each solution were passed through the precleaned conditioned sorbent. The first 10 b.v. were collected separately to ensure column validation. It was found that with the increasing $LiNO_3$ concentration in the solution, the sorption efficiency was significantly reduced. The highest separation factors were observed for 1 mol L^{-1} lithium nitrate solution, showing Ba and Ca reduction on the level of over three magnitude orders and for Sr – over two. The slight decrease in purification efficiency for 4 mol L^{-1} $LiNO_3$ solution is insignificant, considering overall production rate improvement.

Table 3. Separation factors (SF) for MDM-sorbent purification in $LiNO_3$ solution with different molarities.

Separation Factor	K	Sr	Ca	Ba	Pb	Th	U
1 mol L^{-1} $LiNO_3$	0.1	210	60	2,100	>50	≥ 1	≥ 1
4 mol L^{-1} $LiNO_3$	0.1	200	70	1,900	>50	≥ 1	≥ 1
7 mol L^{-1} $LiNO_3$	0.3	4	10	60	>40	≥ 1	≥ 1

Before and after the column, thorium and uranium concentrations were below the detection limit of 6 ppt, indicating no detectable leaching from the sorbent. Apart from Th and U, the potassium concentration value in eluate increased by one order of magnitude. Comparatively higher lithium affinity to manganese oxide than H^+ and K^+ ions [24], along with the high Li-capacity of the MnO_2 [25], explains the eluting of potassium from the sorbent. To make the MDM sorbent purification method applicable to low-background experiments, the sorbent's conditioning procedure and long-term stability were studied further.

Preprints (www.preprints.org) | NOT PEER-REVIEWED | Posted: 8 September 2023 doi:10.20944/preprints202309.0580.v1

So, for further investigation, a 4 mol L^{-1} lithium nitrate solution was selected. After completing the MDM column precleaning and conditioning, as explained in Sect. 2, about 1,000 bed volumes of the $LiNO_3$ solution were passed. The ICP-MS samples were taken every 100-200 bed volume to check the long-term stability of the sorbent and eluting profile of the sorbates. Barium, strontium, and calcium concentrations were used for the indication of column capacity and sorbent's long-time resistance to the highly concentrated solution. The results are presented in Figure 1.

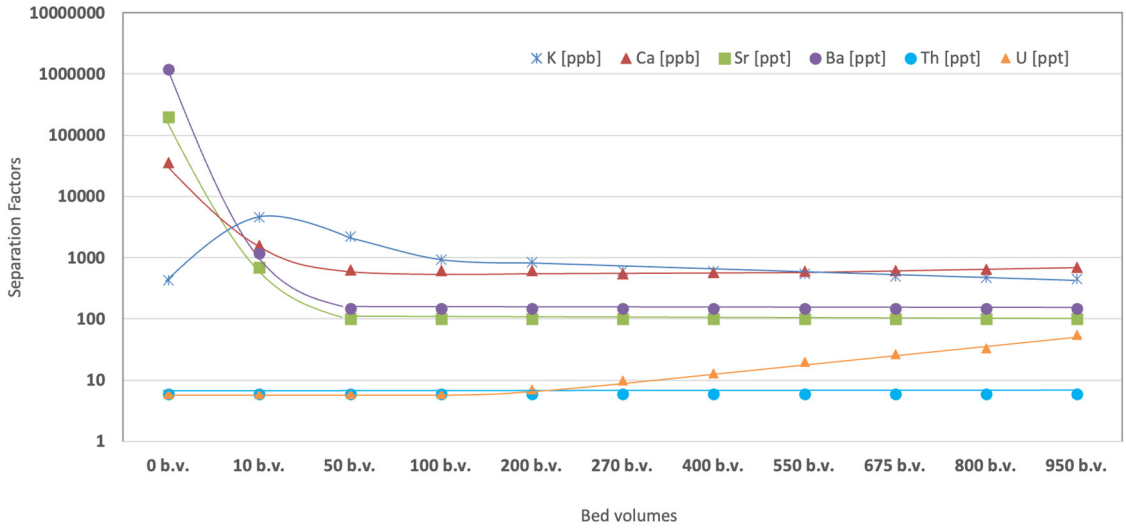

Figure 1. Breakthrough curve of K, Ca, Sr, Ba, Th, and U on MDM sorbent in 4 mol L^{-1} $LiNO_3$ at pH 8.

Within the 10 bed volume of the column purification, the concentration of Sr and Ba was reduced by three orders of magnitude, and within 50 b.v. – by four orders, resulting in a detection limit of about 150 ppt level for both. No breakthroughs were detected till the passing of 950 bed volumes of the solution. Calcium concentration was reduced by two orders of magnitude after passing 50 b.v. of the solution and was stable at about 600 ± 50 ppm till 800 b.v. From 800 b.v. to 950 b.v. calcium concentration increased to about 700 ppb, indicating a 10% breakthrough.

Same as in the study of separation factor as a function of $LiNO_3$ molarity in solution, the K concentration in 50 b.v. increased by one order of magnitude relative to the initial value. Maximum contamination was observed in the first 10 b.v. of the eluate. After the 50 b.v., the potassium leached from the sorbent less but continuously until 950 b.v.

Thorium and uranium concentrations in the initial solution were below the detection limit of 6 ppt, but elution isotherms after the column showed different behavior. While thorium remained at less than six ppt during the procedure, uranium concentration began a slight rise after 200 b.v. and reached 50 ppt level at 950 b.v.

Lithium nitrate crystals were crystallized from the collected purified solution to further investigate the radioactivity reduction with MDM-sorbent purification. The eluate from 50 to 950 b.v. was evaporated twice in a volume and cooled at 4 °C overnight. Obtained crystals (about 60% crystallization efficiency) were dried to remove crystalline water and measured with HPGe (Table 4) and HR-ICP-MS (Table 5). Then, the final lithium carbonate powder was synthesized and tested to understand the applicability of the purification method and the possibility of reaching the projected background level requirements for Li_2CO_3 precursor.

Preprints (www.preprints.org) | NOT PEER-REVIEWED | Posted: 8 September 2023 doi:10.20944/preprints202309.0580.v1

Table 4. The concentration of metallic impurities (HR-ICP-MS) and radioactivity levels (HPGe) measured in final lithium nitrate and lithium carbonate powders.

Element	Concentration [ppb]			Concentration [ppb]	
	Purified $LiNO_3$	Final Li_2CO_3		Purified $LiNO_3$	Final Li_2CO_3
Al	460 ± 50	≤ 300	Mn	180 ± 30	≤ 10
B	110 ± 10	30 ± 5	Na	150 ± 30	50 ± 20
Ba	1.3 ± 0.3	1.0 ± 0.1	Ni	70 ± 20	40 ± 10
Ca	600 ± 120	260 ± 30	Pb	0.20 ± 0.02	0.8 ± 0.2
Cr	60 ± 10	50 ± 10	Sr	≤ 0.2	1.5 ± 0.5
Cs	≤ 10	≤ 10	Th232	≤ 0.01	≤ 0.01
Cu	5 ± 1	4 ± 1	Ti	5 ± 1	3 ± 1
Fe	≤ 80	220 ± 30	U238	0.12 ± 0.02	0.33 ± 0.03
K	2,700 ± 300	300 ± 30	V	≤ 1	≤ 1
Mg	6.3 ± 1.2	1.0 ± 0.2	Zn	500 ± 100	100 ± 10

Table 5. The concentration of metallic impurities (HR-ICP-MS) and radioactivity levels (HPGe) measured in final lithium nitrate and lithium carbonate powders.

	Activity [mBq/kg]	
	Purified $LiNO_3$	Final Li_2CO_3
^{40}K	77 ± 6	≤ 14
^{137}Cs	1.2 ± 0.2	≤ 1.0
^{234}Th	≤ 16	≤ 22
^{234m}Pa	≤ 47	≤ 47
^{226}Ra	≤ 1.0	≤ 1.5
^{228}Ac	≤ 1.4	≤ 1.4
^{228}Th	≤ 1.0	≤ 1.4

The contaminants' concentrations and radioactivities in purified lithium products were compared with those of the initial Li_2CO_3 in Figure 2. The reduction of impurities in purified $LiNO_3$ and final Li_2CO_3 powders were plotted to show their behaviors at different purification stages.

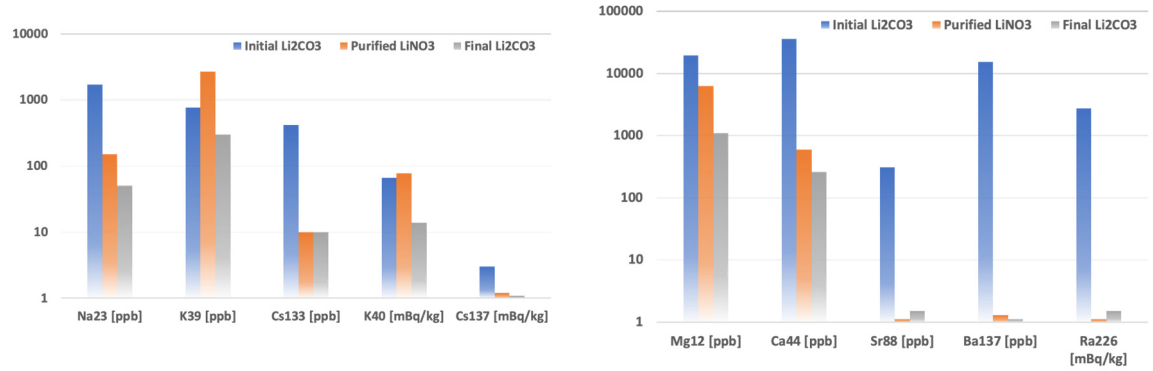

(**a**) (**b**)

Preprints (www.preprints.org) | NOT PEER-REVIEWED | Posted: 8 September 2023 doi:10.20944/preprints202309.0580.v1

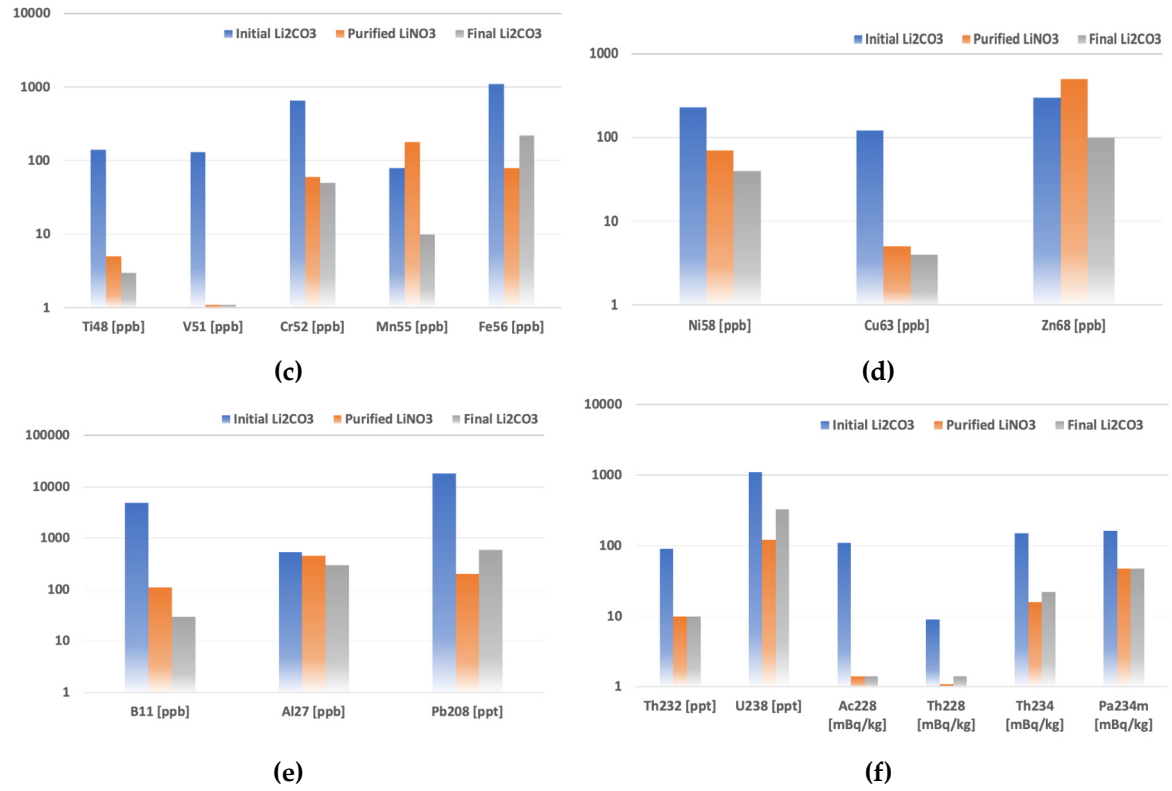

Figure 2. Reduction of impurities in purified $LiNO_3$ and Li_2CO_3 products: (**a**) Removal of ^{23}Na, ^{39}K, ^{133}Cs, ^{40}K, ^{137}Cs; (**b**) Removal of ^{12}Mg, ^{44}Ca, ^{88}Sr, ^{137}Ba, ^{226}Ra; **(c)** Removal of ^{48}Th, ^{51}V, ^{52}Cr, ^{55}Mn, ^{56}Fe; **(d)** Removal of ^{58}Ni, ^{63}Cu, ^{68}Zn; **(e)** Removal of ^{11}B, ^{27}Al, ^{208}Pb; **(f)** Removal of ^{232}Th, ^{238}U and their decay chain products.

According to the reference studies [26,27], in comparison with other types of organic and inorganic sorbents, mixed-valence (III, IV) manganese oxides have relatively high selectivity to Sr^{2+}, Cs^{137+}, and Ra^{2+} in the presence of interfering ions of Mg^{2+}, Ca^{2+}, Na^{+}. However, these sorbents are usually synthesized using $KMnO_4$ and contain a decent amount of potassium in the structure. The purity of the synthesized sorbent is also determined by the purity of raw materials. In the studied 4 mol L^{-1} $LiNO_3$ solution containing Ba, Ca, and Mg on ppm level, the highest separation factors were observed for Ba137 and Ra226. In purified lithium nitrate powder, barium and radium contamination was reduced by four and three orders of magnitude, respectively. Calcium and strontium concentrations decreased by two and three orders of magnitude, while magnesium showed a separation factor of about ten. Ionic radii of Mg^{2+} and Zn^{2+} are very similar to Li^{+} ionic radii [6], making separating these elements difficult [28,29]. Indeed, weak zinc leaching from the sorbent was observed in the lithium nitrate sample. Together with zinc, leaching of K and Mn, matrix components of the sorbent, was found on the level of one order of magnitude. The initial cesium contamination was comparatively low. However, the ICP-MS and HPGe confirmed the reduction to about one mBq/kg. Sodium concentration reduced from ppm to ppb level, showing similar behavior with Cs.

The MDM sorbent purification combined with the co-precipitation method covers a wide range of contaminants. Slight calcium and strontium contamination coming from the Ca-based co-precipitation carrier was eliminated by further sorbent purification. In two purification steps overall, the boron contamination that often accompanies lithium was eliminated by a factor of 50, while no reduction of aluminum was observed. Other tested heavy and transition metals were reduced by one or two orders of magnitude, resulting in the required sub-ppm level. Based on ICP-MS analysis, thorium and uranium contamination was eliminated at the co-precipitation step, and no further contamination for Th was observed in sorbent purification. Apart from thorium, uranium was slightly leached from the sorbent, causing secondary contamination of the solution.

 doi:10.20944/preprints202309.0580.v1

For the final lithium molybdate crystal synthesis, lithium nitrate could not be used and needed to be converted into lithium carbonate. The technical performance of bubbling NH_3 and CO_2 is comparatively complicated, so the sludge of ammonium bicarbonate taken in a stoichiometric amount was used for Li_2CO_3 synthesis. Commercial ammonium bicarbonate is usually radiochemically pure because it is produced from gaseous NH_3 and CO_2. The co-precipitation step with a Li_2CO_3-based carrier was also introduced to eliminate the secondary K, Mn, and Zn contamination from the sorbent. The suggested procedure improved the purity of the final Li_2CO_3 product. Additionally, Na, K, Mg, Mn, and Zn were reduced by one order of magnitude. At the same time, a slight increase in Fe, Pb, and U concentrations was observed, which could be explained by cross-contamination from ammonium bicarbonate and the preconcentration of impurities on the surface of the freshly produced powder.

5. Conclusions

Purifying lithium carbonate for use in low-radioactive background experiments is challenging. The expected issue with potassium removal was accompanied by high radium contamination. Looking at commercial production technology [30], lime (CaO) is one route in which many impurities can find their way into lithium products, notably radium, which commonly occurs in limestone. Combining co-precipitation with inorganic salt-based carriers and sorption with inorganic sorbents is an efficient tool for removing a wide range of chemical and radioactive impurities from lithium salts.

Lithium nitrate was used as an intermediate water-soluble compound for the purification procedure. Carbonate-based carriers were found to be less efficient in the removal of uranium. In the absence of interfering carbonate anion, uranium, thorium, and potassium were removed efficiently with the calcium molybdate-based carrier. The residues of calcium and strontium in the solution were eliminated together with radium in the following MDM sorbent purification. The $LiNO_3$ concentration of 4 mol L^{-1} was selected for sorption purification at pH 8. Long-term operation-wise, the sorbent was stable, and the calcium 10% breakthrough was observed only after passing 950 bed volumes of the solution. Potassium, manganese, zinc, and uranium were leached into the solution from the sorbent, causing secondary contamination. The additional step of co-precipitation (with Li_2CO_3) before synthesizing the final lithium carbonate product was efficient in eliminating the cross-contamination coming from K, Mn, and Zn. However, uranium was not removed with a small amount of the co-precipitate and was preconcentrated with the final product.

Following the suggested purification procedure, all chemical impurities were reduced to the required levels. Radium was reduced by three orders of magnitude, resulting in a satisfactory level of about one mBq/kg. Despite cross-contamination with sorbent's matrix components, K concentration was reduced below the required 0.5 ppm. The ICP-MS and HPGe confirmed the potassium reduction by a factor of two, as a minimum. Thorium was easily removed below 10 ppt at the beginning of the process, and no secondary contamination was observed further. Relatively, for the initial commercial powder, uranium activity was reduced by a factor of three in the final product. However, we could not reach the required uranium level due to the difficulty of its separating in the presence of carbonate anion. Efficient in uranium removal, CMO-based carriers could not be used at the final steps to avoid Ca and Sr cross-contamination. Additional purification steps must be implemented to eliminate the U contamination from the sorbent, for example, ultrafiltration, using chelating or ion exchange resins, recrystallization of the final Li_2CO_3 via carbonization method, etc.

Production efficiency-wise, the MDM sorbent is highly efficient, with over 900 bed volumes of 4 mol L^{-1} $LiNO_3$ solution that could be purified. The method could be useful for low-level background experiments and lithium production in the nuclear industry [31], in Li-ion battery recycling [32], low radioactive water and seawater treatment, etc.

Author Contributions: Conceptualization, methodology, writing—original draft preparation, O.G. and V.M; investigation, validation, technical performance, P.A., Y.K., K.S., H.Y.; ICP-MS analysis, J.C.; HPGe analysis, E.K.L.; supervision, M.H.L.; project administration, funding acquisition, Y.K.; writing—review and editing, all authors. All authors have read and agreed to the published version of the manuscript.

Funding: This work was supported by the Institute for Basic Science (IBS), funded by the Ministry of Science and ICT, Korea (Grant id: IBS-R016-D1).

Data Availability Statement: The authors confirm that all of the data in the article have not been published elsewhere and are available in the article itself.

Acknowledgments: The authors are pleased to acknowledge the support of the SEASTAR™ analytical laboratory for the performance of HR-ICP-MS analysis of the samples.

Conflicts of Interest: The authors declare no conflict of interest.

References

1. Peiro, L.T.; Méndez, G.V.; Ayres, R.U. Lithium: Sources, Production, Uses, and Recovery Outlook. *JOM* **2013,** *65*, 986–996.
2. Oliviera, G.A.D.; Bustillos, J.O.; Ferreira, J.C.; Bergamaschi, V.S.; Moraes, R.M.D.; Gimenez, M.P.; Miyamoto, F.K.; Seneda, J.A. Applications of lithium in nuclear energy. International Nuclear Atlantic Conference -INAC 2017, Belo Horizonte, MG, Brazil, 22–27 October 2017.
3. William, B. Heroy. Disposal of radioactive waste in salt cavities. In *The Disposal of Radioactive Waste on Land.* National Research Council (US) Committee on Waste Disposal. Washington (DC): National Academies Press (US), 1957.
4. Forsberg, C.W.; Lam, S.; Carpenter, D.M; Whyte, D.G.; Scarlat, R.; Contesu, C.; Wei, L.; Stempien, J.; Blandford, E. Tritium Control and Capture in Salt-Cooled Fission and Fusion reactors: Status, Challenges, and Path Forward. *Nucl. Technol.* **2017,** *197*, 119–139.
5. Halfon, S.; Paul, M.; Arenshtam, A.; Berkovits, D.; Bisyakoev, M.; Eliyahu, I.; Feinberg, G.; Hazenshprung, N.; Kijel, D.; Nagler, A.; Silverman, I. High-power liquid-lithium target prototype for accelerator-based boron neutron capture therapy. *Appl. Radiat. Isot.* **2011,** *69*, 1654–1656.
6. Haynes, W.M.; Lide, D.R.; Bruno, T.J. CRC Handbook of Chemistry and Physics: A Ready-reference Book of Chemical and Physical Data. Boca Raton, Florida, CRC Press, 2016.
7. Rahaman, S.; Elomaa, V.-V.; Eronen, T.; Hakala, J.; Jokinen, A.; Julin, J.; Kankainen, A.; Saastamoinen, A.; Suhonen, J.; Weber, C.; Äystö, J. Q values of the ^{76}Ge and ^{100}Mo double-beta decays. *Phys. Lett. B* **2008,** *662*, 111–116.
8. Augier, C.; Barabash, A.S.; Bellini, F.; Benato, G.; Beretta, M.; et al. Final results on the 0νββ decay half-life limit of ^{100}Mo from the CUPID-Mo experiment. Eur. Phys. J. C **2022**, *82*, 1033.
9. Kim, B.H.; Ha, D.H.; Jeon, J.A.; Jo, S.H.; Kang, W.G.; et al. Status and Performance of the AMoRE-I Experiment on Neutrinoless Double Beta Decay. *J. Low Temp. Phys.* **2022,** *209*, 962–970.
10. Yoomin, O. AMoRE [Conference presentation]. NEUTRINO 2022, Virtual Seoul, Korea, May 30 – June 4, 2022.
11. Alenkov, V.; Aryal, P.; Beyer, J.; Boiko, R.S.; Boonin, K.; et al. Technical Design Report for the AMoRE 0νββ Decay Search Experiment. arXiv:1512.05957, 2015.
12. Son, J.K.; Choe, J.S.; Gileva, O.; Hahn, I.S.; Kang, W.G.; Kim, D.Y.; Kim, G.W.; Kim, H.J.; Kim, Y.D.; Lee, C.H.; Lee, E.K.; Lee, M.H.; Leonard, D.S.; Park, H.K.; Park, S.Y.; Ra, S.J.; Shin, K.A. Growth and development of pure Li_2MoO_4 crystals for rare event experiment at CUP. *JINST* **2020,** *15*, C07035.
13. Grigorieva, V.; Shlegel, V.; Bekker, T.; Ivannikova, N.; Giuliani, A.; Marcillac, P.D.; Marnieros, S.; Novati, V.; Olivieri, E.; Poda, D.; Nones, C.; Zolotarova, A.; Danevich, F. Li_2MoO_4 Crystals Grown by Low-Thermal-Gradient Czochralski Technique. *J. Mater. Sci. Eng. B* **2017,** *7*, 63–70.
14. Yeon, H.; Choe, J.S.; Gileva, O.; Hahn, K. I.; Kang, W.G.; Kim, G.W.; Kim, H.J.; Kim, Y.; Kim, Y.; Lee, E.K.; Lee, M.H.; Leonard, D.S.; Milyutin, V.; Park, H.K.; Park, S.-Y.; Shin, K.A. Preparation of low-radioactive high-purity enriched $^{100}MoO_3$ powder for AMoRE-II experiment. *Front. Phys.* **2023,** *11*, 1142136.
15. Armengaud, A.; Augier, C.; Barabash, A.S.; Beeman, J.W.; Bekker, T.B.; et al. Development of ^{100}Mo-containing scintillating bolometers for a high-sensitivity neutrinoless double-beta decay search. *Eur. Phys. J. C* **2017,** *77*, 785.
16. CUP Center for Underground Physics. Available online: https://centers.ibs.re.kr/html/cup_en/ (accessed on 11.07.2023).
17. Novosibirsk Rare Metal Plant. Available online: http://cesium.ru (accessed on 11.07.2023).
18. Gileva, O.; Aryal, P.; Karki, S.; Kim, H.J.; Kim, Y.; Milyutin, V.; Park, H.K.; Shin, K.A. Investigation of the molybdenum oxide purification for the AMoRE experiment. *J. Radioanal. Nucl. Chem.* **2017,** *314*, 1695–1700.

19. Nekrasova, N.A.; Milyutin, V.V.; Kaptakov, V.O.; Kozlitin, E.A. Inorganic Sorbents for Wastewater Treatment from Radioactive Contaminants. *Inorganics* **2023,** *11*, 126.
20. Seastar Chemicals. Available online: https://www.seastarchemicals.com/our-development/specialized-analysis/ (accessed on 12.07.2023).
21. Lee, M.H. Radioassay and Purification for Experiments at Y2L and Yemilab in Korea. *J. Phys.: Conf. Ser.* **2020,** *1468*, 012249.
22. Ryabtsev, A.D.; Kotsupalo, N.P.; Kurakov, A.A.; Menzheres, L.T.; Titarenko, V.I. Theoretical Foundations of Technology for the Production of Lithium Carbonate by the Ammonia Method. *Theor. Found. Chem. Eng.* **2018,** *53*, 815–820.
23. Mühr-Ebert, E. L.; Wagner, F.; Walther, C. Speciation of uranium: Compilation of a thermodynamic database and its experimental evaluation using different analytical techniques. *Appl. Geochem.* **2019,** *100*, 213–222.
24. Koyanaka, H.; Matsubaya, O.; Koyanaka, Y.; Hatta, N. Quantitative correlation between Li absorption and H content in manganese oxide spinel λ-MnO_2. *J. Electroanal. Chem.* **2003,** *559*, 77–81.
25. Murphy, O.; Haji, M.N. A review of technologies for direct lithium extraction from low Li^+ concentration aqueous solutions. *Front. Chem. Eng*. **2002,** *4*, 1008680.
26. Kozlovskaia, O.N.; Shibetskaia, I.G.;, Bezhin, N.A.;, Tananaev, I.G. Estimation of ^{226}Ra and ^{228}Ra Content Using Various Types of Sorbents and Their Distribution in the Surface Layer of the Black Sea. *Materials (Basel).* **2023**, *16*, 1935.
27. Ivanets, A.I.; Prozorovich, V.G.; Kouznetsova, T.F.; et al. Sorption behavior of ^{85}Sr onto manganese oxides with tunnel structure. *J. Radioanal. Nucl. Chem.* **2018,** *316*, 673–683.
28. Sun, Y.; Wang, Q.; Wang, Y.; Yun, R.; Xiang, X. Recent advances in magnesium/lithium separation and lithium extraction technologies from salt lake brine. *Sep. Purif.* **2021**, *256*, 117807.
29. Tansel, B. Significance of thermodynamic and physical characteristics on permeation of ions during membrane separation: Hydrated radius, hydration free energy and viscous effects. *Sep. Purif.* **2012**, *86*, 119–126.
30. Kelly, J.C.; Wang, M.; Dai, Q.; Winjobi, Q. Energy, greenhouse gas, and water life cycle analysis of lithium carbonate and lithium hydroxide monohydrate from brine and ore resources and their use in lithium ion battery cathodes and lithium ion batteries. *Resour. Conserv. Recycl.* **2021,** *174*, 105762.
31. Andrade, M.A.; Oliveira, G.C.; Cotrim, M.E.B.; Seneda, J.A.; Bustillos, O.V. Use of the Ion Exchange Technique for Purifiation of Lithium Carbonate for Nuclear Industry. 2021 International Nuclear Atlantic Conference – INAC 2021, Brazil, November 29 – December 2, 2021.
32. Peng, C.; Liu, F.; Wang, Z.; Wilson, B.P.; Lundström M. Selective extraction of lithium(Li) and preparation of battery grade lithium carbonate (Li_2CO_3) from spent Li-ion batteries in nitrate system. *J. Power Sources* **2019,** *415*, 179–188.